EPJ Web of Conferences **56**, 01008 (2013)
DOI: 10.1051/epjconf/20135601008
© Owned by the authors, published by EDP Sciences, 2013

Impact of carbonation on the durability of cementitious materials: water transport properties characterization

M. Auroy[1,a], S. Poyet[1], P. Le Bescop[1] and J-M. Torrenti[2]

[1] CEA, DEN, DPC, SECR, Laboratoire d'Etude du Comportement des Bétons et des Argiles, F-91191 Gif-sur-Yvette, France
[2] Université Paris-Est, IFSTTAR, Département Matériaux & Structures, 14-52 Boulevard Newton, F-77447 Marne la Vallée Cedex 2, France

Abstract. Within the context of long-lived intermediate level radioactive waste geological disposal, reinforced concrete would be used. In service life conditions, the concrete structures would be subjected to drying and carbonation. Carbonation relates to the reaction between carbon dioxide (CO_2) and the main hydrates of the cement paste (portlandite and C-S-H). Beyond the fall of the pore solution pH, indicative of steel depassivation, carbonation induces mineralogical and microstructural changes (due to portlandite and C-S-H dissolution and calcium carbonate precipitation). This results in the modification of the transport properties, which can impact the structure durability. Because concrete durability depends on water transport, this study focuses on the influence of carbonation on water transport properties. In fact, the transport properties of sound materials are known but they still remain to be assessed for carbonated ones. An experimental program has been designed to investigate the transport properties in carbonated materials. Four hardened cement pastes, differing in mineralogy, are carbonated in an accelerated carbonation device (in controlled environmental conditions) at CO_2 partial pressure of about 3%. Once fully carbonated, all the data needed to describe water transport, using a simplified approach, will be evaluated.
Keywords: carbonation, durability, water transport, hardened cement paste.

1 Introduction

In the framework of the waste geological disposal of long-lived intermediate level radioactive, cement-based materials would be commonly used as construction material for disposal cells as well as containers. Due to the waste thermal output, which can impact the durability of reinforced concrete structures, disposal cells would be ventilated. In these conditions, the ventilation system would maintain the CO_2 partial pressure within the disposal cell; subjecting the structures to simultaneous drying and carbonation over a time span of about 100 years (period during which geological disposal should be "reversible").
Carbonation is one of the main factors in concrete deterioration. It results in the neutralisation reaction of the cement hydrates by CO_2 (acid attack) in accordance with eqs (1-2):

[a] E-mail: martin.auroy@cea.fr

This is an Open Access article distributed under the terms of the Creative Commons Attribution License 2.0, which permits unrestricted use, distribution, and reproduction in any medium, provided the original work is properly cited.

Article available at http://www.epj-conferences.org or http://dx.doi.org/10.1051/epjconf/20135601008

$$Ca(OH)_2(s) + H_2CO_3(aq) \rightarrow CaCO_3(s) + 2H_2O(l) \quad (1)$$

$$CaO_xSiO_{2y}H_2O_z(s) + xCO_2(aq) \rightarrow xCaCO_3 + ySiO_2.tH_2O(s) + (x - t + z)H_2O(l) \quad (2)$$

Eqs (1-2) indicate that carbonation causes the precipitation of calcium carbonate ($CaCO_3$) and the dissolution of the main hydrates, namely portlandite ($Ca(OH)_2$) and calcium silicate hydrates ($C-S-H$). This results in the fall of the pore solution pH and subsequent steel depassivation which is a necessary condition for reinforcement corrosion. It also results in the modification of the carbonated zone physical properties such as those related to transport. Literature data are limited and often conflicting. Calcium carbonate precipitation leads to the reduction of total porosity (clogging) and generally leads to changes in transport properties [1]. It was however observed that despite porosity clogging, carbonation can also alter the pore size distribution (and increase capillary porosity) [2-4] resulting in the increase in transport properties [2].

Reinforced concrete structure durability is greatly influenced by water (see for instance [5]): water is necessary for chemical reactions to occur and can significantly impact concrete transport properties. The durability assessment of concrete structures thus necessitates an accurate description of water transport all along their service life. In this context, the main point of this study aims to experimentally describe the water transport properties of carbonated materials. Based on the results obtained, the second objective aims at developing a physical model connecting mineralogical, microstructural and macroscopic changes.

2 Background

Water transport can be efficiently described using a single equation that accounts for liquid water transport driven by a pressure gradient (3). The other motions (gaseous diffusion and permeation) are neglected. This simplified approach was validated by several authors [6-7] for low-permeability materials:

$$\emptyset\left(\frac{\partial S}{\partial P}\right)\frac{\partial P}{\partial t} = div\left[\frac{K_e}{\eta}grad(P)\right] \quad (3)$$

where $\emptyset$ is the concrete porosity (without unit); S is the saturation index (fraction of the pore volume occupied by water, without unit), it ranges between 0 (dry state) and 1(saturated state); P is the liquid water pressure (Pa); K_e is the unsaturated effective permeability to water (m^2), it reflects the ability of the saturated concrete to transmit water under a pressure gradient and η is the water viscosity (Pa·s).

According to eq. (3), the description of water transport within concrete requires knowledge of:

- the concrete porosity $\emptyset$,
- the left-hand term $\left(\frac{\partial S}{\partial P}\right)$, which is deduced from the water retention curve [8-9],
- the unsaturated effective permeability K_e.

Concrete porosity is easy and quick to measure; it is usually obtained by drying saturated samples until constant weight whereas the water retention curve is more difficult to obtain. These experiments describe the concrete state equilibrium according to the external relative humidity (RH). By using Kelvin-Laplace's law, the RH at equilibrium is converted into water pressure P (eq. (4)). The capillary-pressure curve $P=P(S)$ (or alternatively $S=S(P)$) is then obtained.

$$P(h) = -\rho_w \frac{RT}{M_w} ln(h) \quad (4)$$

where ρ_w is the liquid water density, R the perfect gas constant (8.314 J/mol/K), T the absolute temperature (K), M_w the liquid water molar mass (g.mol^{-1}) and h the relative humidity.

The van Genuchten expression (eq. (5)) is commonly used to fit the results. The prefactor $\left(\frac{\partial S}{\partial P}\right)$ is obtained by differentiation of eq. (5).

$$S(P) = \left[1 + \left(\frac{P}{P_0}\right)^{\frac{1}{1-m}}\right]^{-m} \quad (5)$$

where P_0 (equivalent to a pressure, in Pa) and m (without unit) are the two positive parameters obtained by fitting.

Unsaturated water transport properties are very inconvenient to assess experimentally either using Boltzmann transformation [10] or cup-method [11]. These properties are almost always evaluated using inverse analyses on the basis on isothermal mass variation measurements [7-12]. By doing so, analytical models are commonly used; the first of them being the so-called Mualem-van Genuchten model [13-14].

3 Materials

3.1 Composition

In this study, four different hardened cement pastes are being used:

- a European CEM I which is an Ordinary Portland Cement (96% clinker + 4% gypsum) from Lafarge (Val d'Azergues, France);
- a European CEM III/A which is a binary blend (39% clinker + 61% slag) from Holcim (Héming, France);
- a European CEM V/A, which is a commercial ternary blend (50% clinker + 25% slag + 25% fly ash) from the Calcia (Airvault, France);
- a handmade low-pH mix which is a ternary blend of 40% CEM I (Lafarge Le Teil, France) + 30% fly ash (EdF, Cordemais power plant, France) + 30% silica fume (Condensil S95-DM, France) + 1% superplasticizer (Chrysofluid Optima 175).

All the formulations outlined above are mixed with a water-to-binder ratio of 0.40. This value was chosen because it appeared to yield good properties of the fresh pastes (good workability, neither visible segregation nor bleeding). The CEM I and CEM V are selected by the French National Agency for Nuclear Waste Management (Andra) for their reference formulations for the construction of geological disposal structures and waste packages. The CEM III is selected by Andra for other potential nuclear waste management applications. The low-pH binder is designed by Cau Dit Coumes et al. [15] and Codina et al. [16] mainly to mitigate the chemical interaction between clay minerals and concrete parts which could impair clay physical and chemical properties. Note that the CEM I, CEM V and low-pH mix were already evaluated in a previous study [17] that yielded the water transport properties of the uncarbonated materials.

3.2 Samples preparation

The samples are poured into polypropylene cylindrical molds of 100 mm height and 50 mm diameter. They are unmolded two weeks after casting and then cured for four months in sealed containers. The CEM I, CEM III and CEM V samples are kept immersed in a special curing solution

whose composition is designed to prevent calcium and alkalis leaching [18]. The pore-solution is expressed at high-pressure [19-20] and analyzed using ionic chromatography (Table 1).

Table 1: Ion chromatography results for the pore solutions of CEM I, CEM III and CEM V pastes: the results are given in mmol/L.

Cations	CEM I	CEM III	CEM V
Na^+	47	143	87
K^+	452	292	533
Ca^{2+}	2	2.5	2

The pore-solution of the low-pH materials is known to exhibit important changes during the early months of hydration [16], a different protocol is then chosen: several samples are reduced into a rough powder and added to deionized water to generate the curing solution.

The top and bottom parts of the samples which are known to present different properties as the bulk [21-22] are cut off and discarded. The thickness of the removed parts is assessed using accelerated chemical degradation [23] and set to 10 mm. Samples are immersed in ammonium nitrate (6M). The leaching solution is stirred constantly but is not renewed. After one month, the samples are withdrawn from the solution, sawn in two parts and sprayed with phenolphthalein solution. Three zones were then visible (Figure 1):

- the central part of the sample, where the degradation depth is homogeneous versus height,
- the bottom of the sample, the degradation depth is less due to sedimentation,
- the top part of the sample, where the degradation depth is the higher due to bleeding.

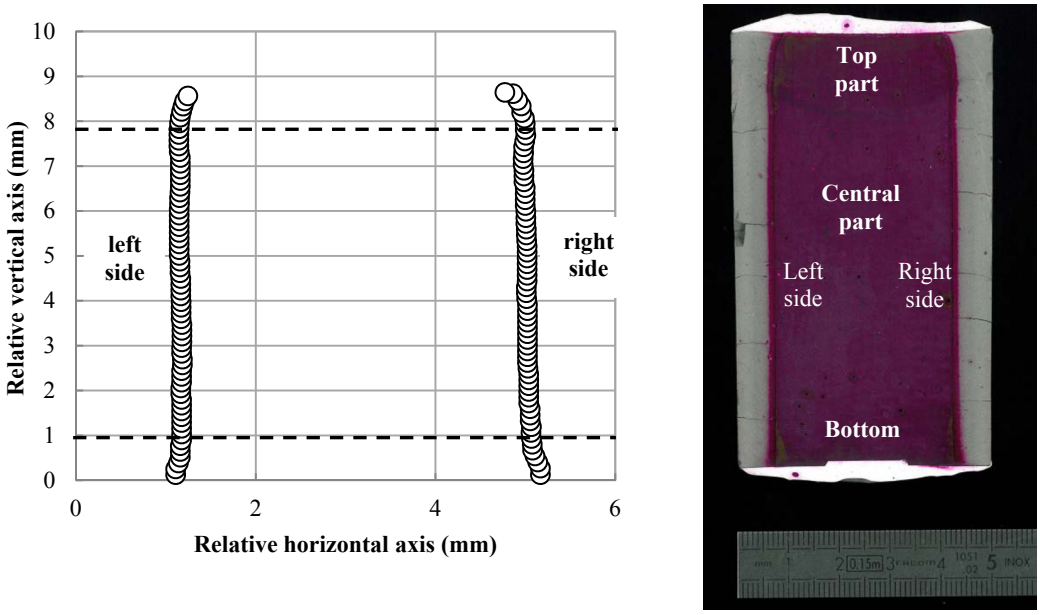

Figure 1: Degradation profile of CEM I paste sample after 1 month in ammonium nitrate (6M) at ambient temperature

The removal of top and bottom ends is believed to yield homogeneous properties versus height. 6 mm-thick disks are sawn from the central part of the resulting samples (Figure 2).

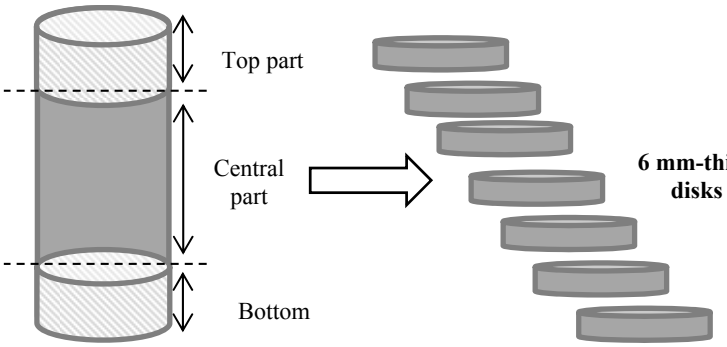

Figure 2: Sample cutting pattern

4 Accelerated carbonation

The disks were kept at 25°C and 55% RH for one month before carbonation. The carbonation tests are performed in the following environmental conditions:

- CO_2 content of 3% ($P_{CO_2} \approx 3$ kPa). This value was shown to ensure representativeness of the mineralogical evolution compared to atmospheric carbonation [24].
- 25°C and 55% RH. According to several authors [25-27], the carbonation speed is optimal for intermediate RHs, i.e. high enough to allow CO_2 solubilisation and sufficiently low to not slow down the CO_2 diffusion.

The tests are performed in an accelerated carbonation device [17], which is composed of two major parts (Figure 3):

- a commercial environmental chamber which allows controlling temperature and RH,
- a specific CO_2 control/regulation device that continuously measures the CO_2 content within the chamber (using infrared absorption) and injects CO_2 whenever the measured value falls below the prescribed one.

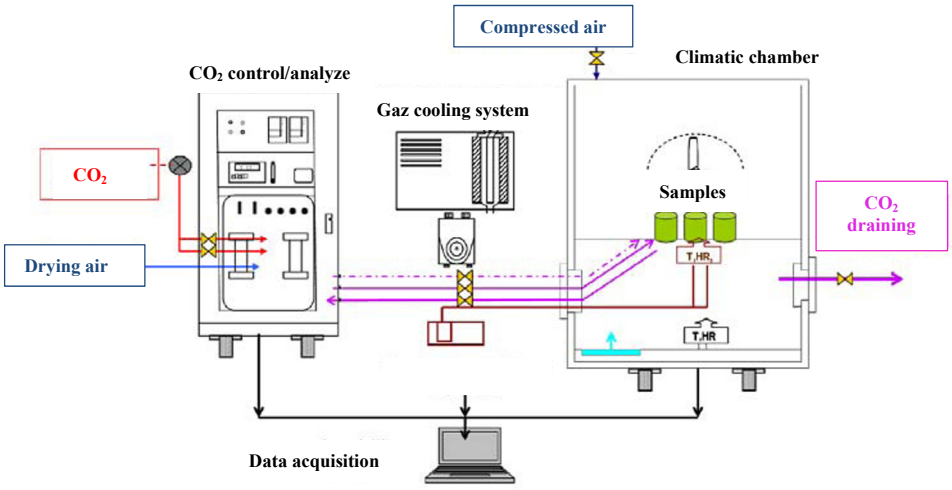

Figure 3: Schematic view of the aaccelerated carbonation device [17]

The time needed to achieve complete carbonation of the 6 mm thick CEM I disks is estimated using preliminary tests. Disks of CEM I paste (w/b = 0.40, thickness = 5 mm) are submitted to 3% CO_2 for 130 days at 25°C and 55% RH. The progress of carbonation progress is monitored by periodic weighing but full carbonation state could not be reached (Figure 4). Considering the results obtained

by Castellote et al. [24] (using similar materials and environmental conditions, Figure 4), the time needed to reach full carbonation (i.e. constant mass) disks is estimated according to the disk thickness (Figure 5) with the expression (6):

$$t(e) = t(e = 5\ mm) \times \left(\frac{e}{5\ mm}\right)^2 \quad (6)$$

where $t(e)$ is the time needed to reach full carbonation of a e thick CEM I disk, and $t(e = 5\ mm)$ is the time needed to reach full carbonation of a 5 mm thick CEM I disk.

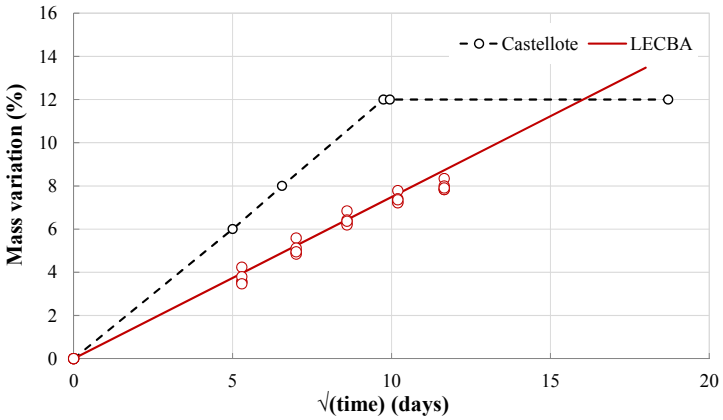

Figure 4: Mass variation of CEM I samples during accelerated carbonation test at 3% CO_2 content (22°C, 65% RH) (dotted line) [23] – Mass variation of CEM I samples during accelerated test, in LECBA, at 3% CO_2 content (25°C, 55% RH) (straight line)

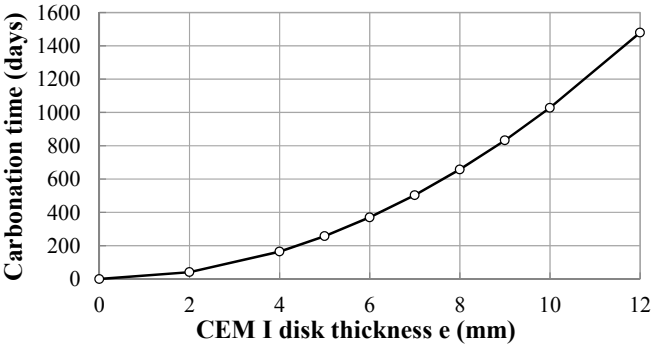

Figure 5: Carbonation time evaluation of CEM I disk according to its thickness

The time needed to reach full carbonation for our 6 mm is evaluated to be about one year. Note that the other studied formulations (CEM III, CEM V and Low-pH) will require a shorter time period to reach complete carbonation because of their reduced portlandite content in relation to clinker substitution by pozzolanic additions (cf. part 3.1).

Changes induced by carbonation (cf. part 1) can be described using classical tools: the first of them being the well-known phenolphthalein solution spraying. Phenolphthalein is a pH indicator which turns pink in the uncarbonated zone and remains colorless in the carbonated one. This technique is easy to implement, although not accurate (it underestimates the carbonated depth). It does not allow quantifying portlandite dissolution and identifying the mineralogical evolution. It is therefore appropriate to complement using alternative analytical techniques such as X-Ray Diffraction (XRD) for mineralogical identification and ThermoGravimetric Analysis (TGA) for quantification.

5 Water transport

5.1 Porosity

The porosity of the carbonated pastes is obtained by oven-drying of initially saturated samples. 80°C (with $CaCl_2$) was chosen as the reference temperature in order to enable comparison with the previous study of Drouet [17].

5.2 Water retention

The water retention curve of the carbonated pastes is characterized using the desiccator method [28]. Initially saturated carbonated paste samples are put in closed desiccators above saturated salt solutions that control RH (in isothermal conditions). Periodically the desiccators are opened and the sample weights measured. The mass loss at equilibrium (constant mass) for different RH values is enables the evaluation of the water retention curve [8]. Here again, drying at 80°C (with $CaCl_2$) is used as the reference dry state.

5.3 Unsaturated permeability

In our case, the (effective) permeability K_e cannot be evaluated using inverse analysis (cf. part 2) because of the small disk size. The cup-method is alternatively chosen. For these experiments, thin disks (6 millimeters in our case) do constitute a boundary separating two different environments (at the same temperature but with two different RH values: RH_1 and RH_2) through which water is transported (Figure 6). In steady-state, the water flux (J_w) [kg/s], expressed according to Darcy's law (eq. (7)), allows estimating the transport property K_e on the specific RH range [RH_1, RH_2] (eq. (8)).

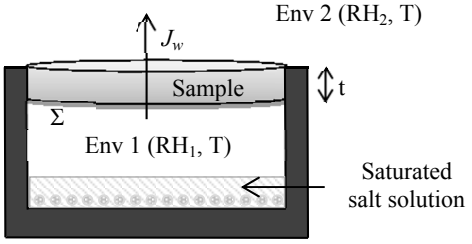

$$J_w = -\rho_w \frac{K_e}{\eta} grad(P) \qquad (7)$$

Figure 6: Sketch of the cup-method test

Practically speaking, the cup mass variation vs. the time is plotted for a given RH range (Figure 7).

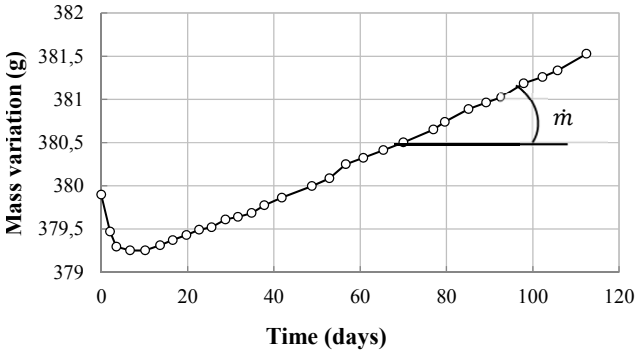

Figure 7: Cup mass evolution vs. time for a 33% (RH_1)-50% (RH_2) RH range at 20°C [11]

Steady-state conditions are reached once mass evolves linearly vs. time. The time required to reach the steady-state is estimated at about 1 month [11]. The effective permeability is estimated using eq. (8).

$$K_e = -\frac{\dot{m}\eta}{\rho\Sigma\frac{\Delta P}{t}} \quad (8)$$

where $\dot{m}$ is the slope of the line (without unit), Σ is the sample surface (m²), t is the thickness (m) and ΔP the pressure variation (Pa).

The cup-method test is repeated on several RH ranges. The experimental test conditions are described in Table 2. Saturated salt solutions are used to control RH_1 (Figure 6). An environmental chamber (temperature and RH controlled) is used to control RH_2 and T (Figure 6).

Table 2: RH range used for the experimental cup-method test [29]

RH_1 (%)	Salt solution	RH_2 (%)
100	Deionised water	95
98	Potassium sulfate	90
93	Potassium nitrate	80
85	Potassium chloride	70
75	Sodium nitrate	60
64	Ammonium nitrate	50
54	Magnesium nitrate	40
43	Potassium carbonate	30
33	Magnesium chloride	20

6 First results

At the time of writing the article, the mineralogical compositions of sound materials were characterized by XRD (Figure 8) and TGA/DTG (Figure 9) analysis.

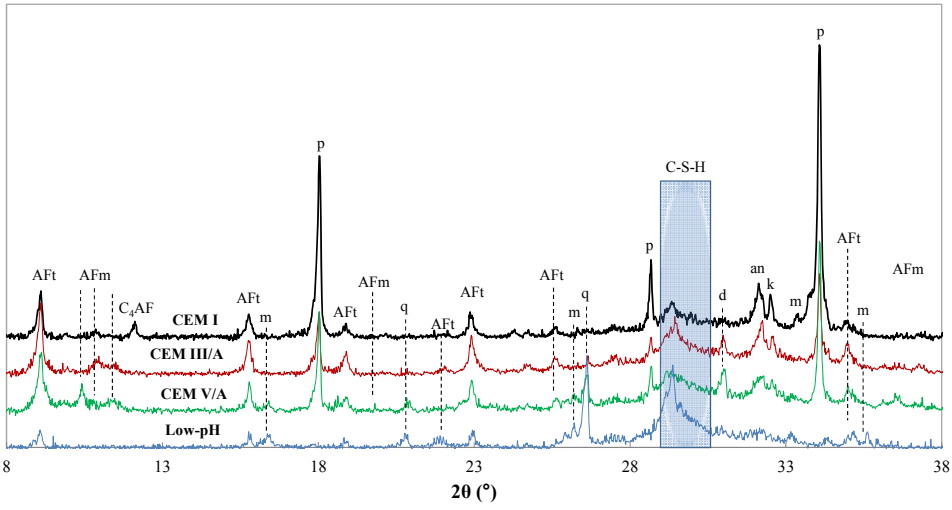

Figure 8 : X-Ray diffractograms of sound materials (CEM I, CEM III/A, CEM V/A and Low-pH) (Aft: ettringite, Afm: monosulfate, C_4AF: ferrite anhydrous phase, m: mullite, p: portlandite, q: quartz, c: calcite, d: dolomite, an: anhydrous phases C_2S et C_3S, k: katoite)

The mineralogical structure of the sound materials is commonly observed for similar materials. According to literature data [30], the obtained X-Ray diffractograms provide good description of mineralogical evolutions during the hydration process. The presence of portlandite, C-S-H, Aft phase, AFm phase, and minor phases is detected.

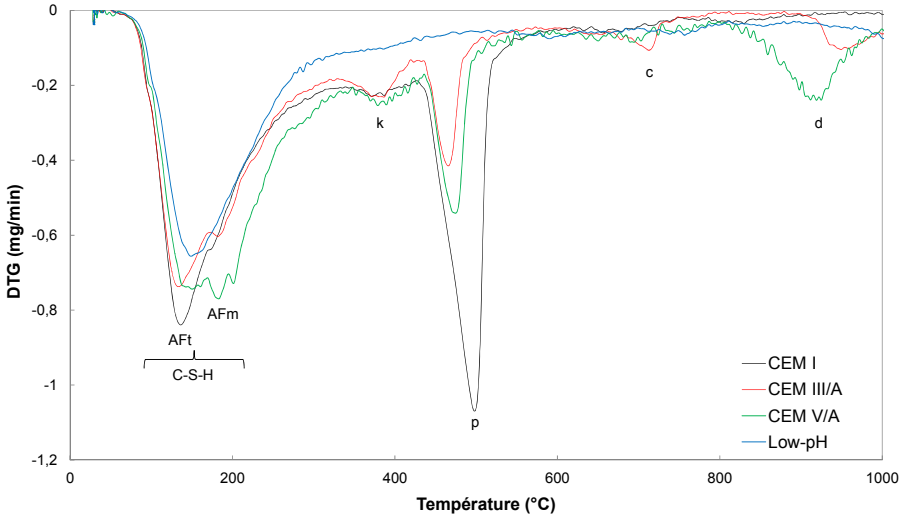

Figure 9: DTG curves of sound materials (CEM I, CEM III/A, CEM V/A and Low-pH) (p: portlandite, k: katoite, c: calcium carbonates, d: dolomite)

Portlandite quantification of sound materials is deduced from TGA/DTG curves (Figure 9). The corresponding values are provided in Table 3.

Table 3: Portlandite quantification (mol/L) of sound materials (CEM I, CEM III/A, CEM V/A and Low-pH (T1)) by TGA/DTG

	CEM I	CEM III	CEM V	Low-pH (T1)
Portlandite (mol/L)	5.3	1.8	2.3	0

The portlandite concentration estimated by TGA/DTG is very close to those determined during the previous study [17]. Note that the initial C-S-H concentration is evaluated from water sorption experiment and the Olson & Jennings method [31]. These experiments are being done. The complete description of sound materials mineralogical compositions will provide the carbonation characterization in a coherent way.

7 Conclusion

Carbonation has great importance for water transport properties in cement based materials. In the context of long-lived intermediate level radioactive waste geological disposal, that is a major issue for the durability of reinforced concrete structures. An experimental program is defined to investigate the carbonation effect on water transport properties. Note that literature data are limited and often conflicting. By using the simplified approach, water transport properties are determined. Practically, four hardened cement pastes of interest for Andra (the French National Agency for Nuclear Waste Management) are carbonated at 3% CO_2 content (25°C, 55% RH) over a time span of about one year (until complete carbonation). All data needed to describe water transport are then determined.

Acknowledgment

The authors would like to thank Xavier Bourbon from the French national agency for radioactive waste management (Andra) for financial support.

References

[1] N. Hyvert, Ph.D. Thesis, Toulouse University, France (2009).
[2] V.T. Ngala and C. L. Page, Cement and Concrete Research **27**, 995-1007 (1997).
[3] Y.F. Houst and F.H. Wittmann, Cement and Concrete Research **24**, 1165-1176 (1994).
[4] M. Thiéry, Ph.D. Thesis, Ecole Nationale des Ponts et Chaussées, France (2005).
[5] K. Tuutti, Swedish Cement and Concrete Research Institute **10**, 468p (1982).
[6] M. Thiery et al., Revue Européenne De Génie Civil 11, 541-77 (2007).
[7] M. Mainguy and O. Coussy, Journal of Engineering Mechanics, 582-92 (2001).
[8] V. Baroghel-Bouny, Cement and Concrete Research **37**, 414-37 (2007).
[9] V. Baroghel-Bouny, Cement and Concrete Research **37**, 438–54 (2007).
[10] L. Pel and K. Kopinga, HERON **41**, 95-105 (1996).
[11] V. Baroghel-Bouny et al., Materials and Structures **30**, 340–48 (1997).
[12] V. Baroghel-Bouny, Cement and Concrete Research **29**, 1225-1238 (1999).
[13] Y. Mualem, Water Resources Research **12**, 513-22 (1976).
[14] M. T. Van Genuchten, Soil Science Society of America Journal **44**, 892-98 (1980).
[15] C. Cau Dit Coumes et al., Cement and Concrete Research **36**, 2152-63 (2006).
[16] M. Codina et al., Cement and Concrete Research **38**, 437-48 (2008).
[17] E. Drouet, Ph.D. Thesis, ENS Cachan, France (2010).
[18] K. Kobayashi et al., Cement and Concrete Research **24**, 55-61 (1994).
[19] R. S. Barneyback and S. Diamond, Cement and Concrete Research **11**, 279-85 (1981).
[20] M. Cyr and A. Daidié, Review of Scientific Instruments **78**, 023906 (2007).
[21] P. C. Kreijger, Materials and Structures **17**, 275–283 (1984).
[22] J. M. Khatib and P. S. Mangat, Cement and Concrete Composites **25**, 97–108 (2003).
[23] F. M. Lea, Magazine of Concrete Research **17**, 115-16 (1965).
[24] M. Castellote et al., Materials and Structures **42**, 515-25 (2008).
[25] G. J. Verbeck, ASTM Special Publication **205**, 17-36 (1958).
[26] M. Vénuat, Annales ITBTP **364**, (1978).
[27] V. G. Papadakis et al., Materials Journal **88**, 363-73 (1991).
[28] L. Wadsö et al. Drying Technology **22**, 2427-40 (2004).
[29] L. Greenspan, Journal of Research of the National Bureau of Standards **81**, 89–96 (1977).
[30] M. Bishop et al., Chemistry of materials **15**, 3074-88 (2003).
[31] R. A. Olson and H. M. Jennings, Cement and Concrete Research **31**, 351-56 (2001).